

Rapporti tecnici

INGV

**On the implementation of
Absorbing Boundary Conditions in a
Finite Difference code with
conventional grid**

122



Direttore

Enzo Boschi

Editorial Board

Raffaele Azzaro (CT)

Sara Barsotti (PI)

Mario Castellano (NA)

Viviana Castelli (BO)

Anna Grazia Chiodetti (AC)

Rosa Anna Corsaro (CT)

Luigi Cucci (RM1)

Mauro Di Vito (NA)

Marcello Liotta (PA)

Lucia Margheriti (CNT)

Simona Masina (BO)

Nicola Pagliuca (RM1)

Salvatore Stramondo (CNT)

Andrea Tertulliani - coordinatore (RM1)

Aldo Winkler (RM2)

Gaetano Zonno (MI)

Segreteria di Redazione

Francesca Di Stefano - coordinatore

Tel. +39 06 51860068

Fax +39 06 36915617

Rossella Celi

Tel. +39 06 51860055

Fax +39 06 36915617

redazionecen@ingv.it



Rapporti tecnici INGV

ON THE IMPLEMENTATION OF ABSORBING BOUNDARY CONDITIONS IN A FINITE DIFFERENCE CODE WITH CONVENTIONAL GRID

Andrea Bizzarri

INGV (Istituto Nazionale di Geofisica e Vulcanologia, Sezione di Bologna)

122

Table of contents

Introduction	5
1. The fault model	6
2. Domain Boundary Conditions	7
2.1. Fixed boundaries	7
2.2. Cyclic boundaries	7
2.3. A compact scheme for implementing ABCs	7
3. Clayton and Engquist ABCs	8
4. Reynolds ABCs	8
5. Emerman and Stephen ABCs	9
6. Higdon ABCs	9
7. Higdon, Clayton and Engquist ABCs	10
8. Liu and Archuleta ABCs	10
9. Peng and Toksöz ABCs	11
10. Summary	12
Acknowledgements	14
References	14

Introduction

Modern numerical experiments for the solution of the direct problem in Seismology (i.e., the elasto–dynamic problem for fault surfaces) require the use of advanced numerical algorithms, capable of capturing all the essential features of the physical problem and to properly resolve the characteristic temporal and spatial lengths. In realistic dynamic models the fault surfaces have dimensions of several kilometer, in both strike and dip directions (e.g., Bizzarri et al., 2009, among many others). The required resolution of the problem typically requires the adoption of spatial sampling of several meter and time steps of the order of fractions of millisecond.

As a consequence, this results in numerical experiments with algebraic equations discretized over hundreds of mega–nodes ($n \times 10^8$ nodes). In turn, in order to obtain results in affordable human–times, this requires the exploitation of symmetry conditions (see for instance Bizzarri, 2009 for further details) and the use of several code optimizations, as well as an efficient parallel programming.

In addition to the grid dispersion phenomenon, intrinsically present in every numerical algorithm, another problem can affect the obtained solutions: the spurious reflections of signals originated from the boundaries of the computational domain. These reflections might introduce numerical artifacts into the computed solutions and constructively interfere, finally causing problematic oscillations.

One way to solve this problem is to arbitrarily enlarge the size of the computational domain — ideally approaching the unbounded (with the exclusion of the free surface) medium — in order to delay the back propagating fronts originating from the model boundaries. This solution is theoretically optimal, but technically unpractical, since the size of the model can easily become larger than the available computational resources.

A second possibility to assess the problem is to introduce some *ad hoc* conditions at (or near to) the boundaries of the computational domain, in order to cause the back propagating waves to be adequately small (ideally null) from a numerical point of view.

In this study we present different numerical algorithms consisting in Absorbing Boundary Conditions (ABCs thereafter) that can be efficiently used to reduce the boundary effects (i.e., the waves originated by a seismogenic fault of finite extension reflected back into the model by the boundaries of the computational domain). We also indicate how they can be proficiently implemented in a Finite Difference, conventional grid numerical FORTRAN code.

1. The fault model

In the following of this work we will consider the fault model described in detail in Bizzarri and Cocco (2005); readers can refer to that work for more information. Here we simply recall the prominent features of that model, as well as the geometry and the conventions. Let us consider, for sake of simplicity, a vertical, planar fault, having dimensions L^f and W^f in the strike and dip direction, respectively. The fault is embedded in a surrounding medium, discretized by mean of specialized parallelepipeds, having faces parallel to the Cartesian axes, x_1 , x_2 and x_3 . Figure 1 illustrates the system geometry.

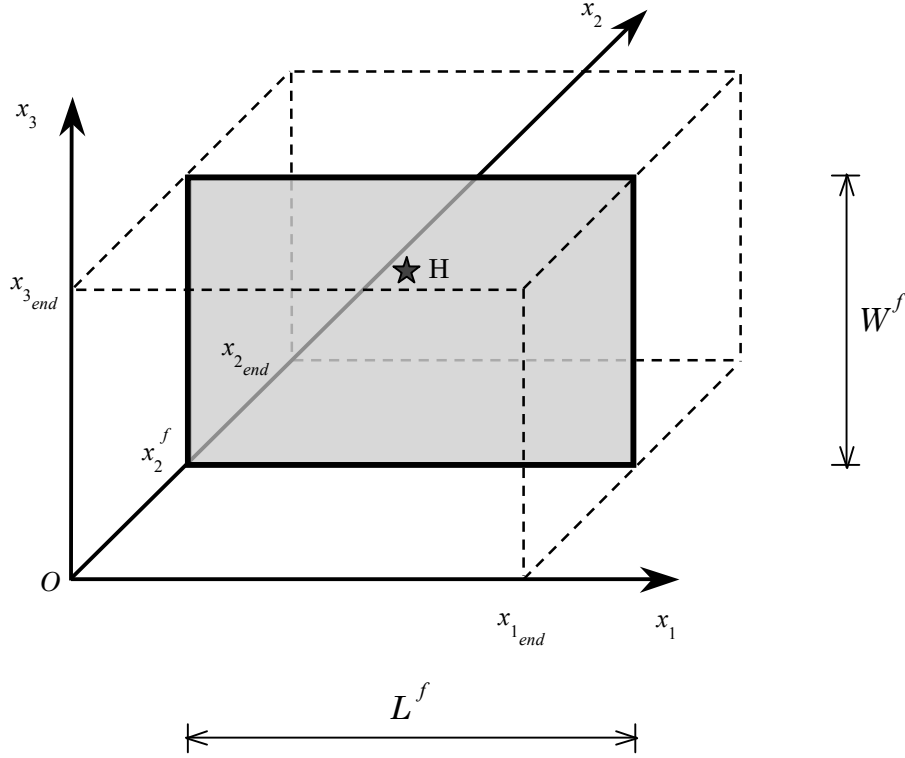


Figure 1. Schematic representation of the fault model considered in the present study. The grey plane $x_2 = x_2^f$ represents the fault, the star H indicates the hypocenter and the dashed lines denote the spatial extension of computational domain, $\Omega^{(FD)}$. x_{1_end} , x_{2_end} and x_{3_end} are the dimensions of $\Omega^{(FD)}$ in each direction. The plane $x_3 = 0$ is the free-of-tractions plane (i.e., the free surface).

In the following we will refer to the FORTRAN code presented in Bizzarri and Cocco (2005), which is a Finite Difference, conventional grid code (in that all components of slip, slip velocity and force are defined at the same node), 2nd order-accurate both in space and in time, both on the fault plane and on the surrounding medium. Explicit time stepping is adopted.

Thereinafter, we will refer to the actual time level by using the integer superscript m ($m = 1, \dots, n_{end}$); the subscript triplet ijk defines a grid node within $\Omega^{(FD)}$ having the absolute coordinates $(x_1(i), x_2(j), x_3(k)) = (i\Delta x_1, (j-1)\Delta x_2, (k-1)\Delta x_3)$, where Δx_1 , Δx_2 and Δx_3 are the spatial sampling along the x_1 , x_2 and x_3 Cartesian axes, respectively. (Incidentally we emphasize that our code fully manages elements with different discretization sizes in each direction.) The particle displacement vector and its time derivative (i.e., the particle velocity vector, or displacement rate vector) will be indicated with symbols \mathbf{U} and $\dot{\mathbf{U}}$, respectively. Each component of such vectors will be denoted with subscript l ($l = 1, 2, 3$). In conclusion, with the compact notation

$$U_{ijk_l}^m$$

we will refer to the l -component of the displacement in the point $(i\Delta x_1, (j-1)\Delta x_2, (k-1)\Delta x_3)$ within the medium, computed at the time level m .

2. Domain Boundary Conditions

2.1. Fixed boundaries

The simplest type of Domain Boundary Condition (DBC henceforth) is represented by the fixed boundary, which has the physical meaning of a fixed wall. The implementation of such a condition is straightforward; for instance, the imposition of the fixed boundary condition in the x_1 direction is simply expressed as follows:

$$\begin{aligned} U_{1jk_l}^m &= 0, & \dot{U}_{1jk_l}^m &= 0 \\ U_{i_{end}jk_l}^m &= 0, & \dot{U}_{i_{end}jk_l}^m &= 0 \end{aligned} \quad (1)$$

where the conditions $\dot{U}_{1jk_l}^m = 0$ and $\dot{U}_{i_{end}jk_l}^m = 0$ formally are Dirichlet and Neumann boundary conditions, respectively. Analogous conditions can be written for other boundaries of the computational domain. We can clearly envisage that when a wave is traveling toward the boundary $x_1 = x_{1_{end}}$ there is an abrupt transition between a non null displacement (and displacement rate) at $x_1 = x_{1_{end}} - \Delta x$ and a null displacement (and displacement rate) at $x_1 = x_{1_{end}}$. Of course, this phenomenon is unphysical and conditions (1) cause spurious reflections that back propagate into the model.

2.2. Cyclic boundaries

Another type DBC is represented by cyclic boundary. Cyclic boundary conditions are applied to a pair of boundaries in which one boundary is reproduced geometrically by revolving or translating the other boundary. This means that boundaries which will be defined as cyclic are identical in every aspect except for their location.

From a practical point of view, the implementation of such a condition implies that a wave which travels, for instance, along the strike direction x_1 and which touches the right end of the domain along this direction ($x_1 = x_{1_{end}}$), instead of being reflected into the model or being absorbed, appears at the beginning of the x_1 axis ($x_1 = \Delta x$). This conditions, of course, does not have a precise physical meaning, but it has been largely implemented in numerical codes devoted to the solution of the elasto-dynamic problem, as a natural consequence of its inherent effortlessness.

Analytically, this condition is expressed as follows (again we will focus on the x_1 axis; the same holds for other directions):

$$\begin{aligned} U_{i_{end}jk_l}^m &= U_{1jk_l}^m \\ \dot{U}_{i_{end}jk_l}^m &= \dot{U}_{1jk_l}^m \end{aligned} \quad (2)$$

2.3. A compact scheme for implementing ABCs

A node belonging to an absorbing plane is a special node of $\Omega^{(FD)}$ for which the Absorbing Boundary Condition (ABC) is applied. We impose the ABCs on each components l of the particle velocity $\dot{\mathbf{U}}$ accordingly to the following analytical compact relation (see Bizzarri and Spudich, 2008 and references therein):

$$\begin{aligned}
\dot{U}_{1jk_l}^m &= A_{01}\dot{U}_{2jk_l}^m + A_{02}\dot{U}_{3jk_l}^m \\
&+ A_{10}\dot{U}_{1jk_l}^{m-1} + A_{11}\dot{U}_{2jk_l}^{m-1} + A_{12}\dot{U}_{3jk_l}^{m-1} \\
&+ A_{20}\dot{U}_{1jk_l}^{m-2} + A_{21}\dot{U}_{2jk_l}^{m-2} + A_{22}\dot{U}_{3jk_l}^{m-2}
\end{aligned} \tag{3}$$

Equation (3) holds for the left boundary $x_1 = 0$ (i.e., $i = 1$). For the right boundary $x_1 = x_{1_{end}}$ (i.e., $i = i_{end}$) the condition (4) becomes:

$$\begin{aligned}
\dot{U}_{i_{end}jk_l}^m &= A_{01}\dot{U}_{i_{end}-1jk_l}^m + A_{02}\dot{U}_{i_{end}-2jk_l}^m \\
&+ A_{10}\dot{U}_{i_{end}jk_l}^{m-1} + A_{11}\dot{U}_{i_{end}-1jk_l}^{m-1} + A_{12}\dot{U}_{i_{end}-2jk_l}^{m-1} \\
&+ A_{20}\dot{U}_{i_{end}jk_l}^{m-2} + A_{21}\dot{U}_{i_{end}-1jk_l}^{m-2} + A_{22}\dot{U}_{i_{end}-2jk_l}^{m-2}
\end{aligned} \tag{4}$$

Equations (3) and (4) can be written in a similar form for the boundaries $x_2 = x_{2_{end}}$, $x_3 = 0$ and $x_3 = x_{3_{end}}$ (we recall here that $x_2 = 0$ is the free surface; see Figure 1). The coefficients $\{A_{pq}\}_{p,q=0,1,2}$ appearing in the previous equations depend on the choice of the specific ABC scheme.

In practice, the first step obviously is the calculation of $\dot{\mathbf{U}}^m$ and \mathbf{U}^m in regular (i.e., internal) nodes, as obtained by the discretized wave equations. Then the particle velocity at time level m is calculated for nodes belonging to absorbing boundary walls, following equations (3) and (4), where values of interior grid points and previous time levels are required to nullify (minimize) unwanted reflections. For nodes belonging to boundary edges $\dot{\mathbf{U}}^m$ is calculated as arithmetic average of values arising from the two walls of which the edges is the intersection. Finally, the values in corners are obtained as arithmetic average of values coming from the three walls that have that corner in common. Updated particle displacement components at actual time level m are derived by numerical integration from updated particle velocity components.

In the next sub-sections will describe in detail the expressions of the coefficients $\{A_{pq}\}_{p,q=0,1,2}$ in equations (3) and (4). We assume that spatial sampling in all direction is Δx ($\Delta x_1 = \Delta x_2 = \Delta x_3 \equiv \Delta x$) and it is constant through the medium (i.e., spatially homogenous mesh).

3. Clayton and Engquist ABCs

Following Clayton and Engquist (1977) we have:

$$\begin{aligned}
A_{00} &= 0 \\
A_{01} &= 0 \\
A_{02} &= 0 \\
A_{10} &= 1 - c\Delta t/\Delta x \\
A_{11} &= c\Delta t/\Delta x \\
A_{12} &= 0 \\
A_{20} &= 0 \\
A_{21} &= 0 \\
A_{22} &= 0
\end{aligned} \tag{5}$$

where c is the velocity of the incident wave and Δt the time step.

4. Reynolds ABCs

Reynolds (1978) expresses the coefficients $\{A_{pq}\}_{p,q=0,1,2}$ as:

$$\begin{aligned}
A_{00} &= 0 \\
A_{01} &= 0 \\
A_{02} &= 0 \\
A_{10} &= 1 - c\Delta t/\Delta x \\
A_{11} &= 1 + c\Delta t/\Delta x \\
A_{12} &= 0 \\
A_{20} &= 0 \\
A_{21} &= -1 - c\Delta t/\Delta x \\
A_{22} &= c\Delta t/\Delta x
\end{aligned} \tag{6}$$

5. Emerman and Stephen ABCs

Emerman and Stephen (1983) demonstrated that the boundary condition of Clayton and Engquist (1977) is unstable for a wide range of parameters (namely, when $v_S/v_P < 0.46$, being v_P and v_S the P and S wave velocities, respectively). They proposed an alternative ABC, which has been proved to be stable for any ratio $v_S/v_P > 0$:

$$\begin{aligned}
A_{00} &= 0 \\
A_{01} &= (\Delta t - \Delta x/c)/(\Delta t + \Delta x/c) \\
A_{02} &= 0 \\
A_{10} &= 2(\Delta x/c)/(\Delta t + \Delta x/c) \\
A_{11} &= 2(\Delta x/c)/(\Delta t + \Delta x/c) \\
A_{12} &= 0 \\
A_{20} &= (\Delta t - \Delta x/c)/(\Delta t + \Delta x/c) \\
A_{21} &= -1 \\
A_{22} &= 0
\end{aligned} \tag{7}$$

6. Higdon ABCs

Following Higdon (1991) the coefficients $\{A_{pq}\}_{p,q=0,1,2}$ are expressed as:

$$\begin{aligned}
A_{00} &= 0 \\
A_{01} &= -(Q_X + R_X) \\
A_{02} &= -Q_X R_X \\
A_{10} &= -(Q_T + R_T) \\
A_{11} &= -(Q_X R_T + Q_T R_X + Q_{XT} + R_{XT}) \\
A_{12} &= -(Q_X R_{XT} + R_X Q_{XT}) \\
A_{20} &= -Q_T R_T \\
A_{21} &= -(Q_T R_{XT} + R_T Q_{XT}) \\
A_{22} &= -Q_{XT} R_{XT}
\end{aligned} \tag{8}$$

where:

$$\begin{aligned}
Q_X &= (W_b(B_{E1} + N_I) - N_I)/(B_{E1} + N_I)/(1 - W_b) \\
R_X &= (W_b(B_{E2} + N_I) - N_I)/(B_{E2} + N_I)/(1 - W_b) \\
Q_T &= (W_b(B_{E1} + N_I) - B_{E1})/(B_{E1} + N_I)/(1 - W_b)
\end{aligned}$$

$$\begin{aligned}
R_T &= (W_b(B_{E2} + N_I) - B_{E1}) / ((B_{E2} + N_I) * (1 - W_b)) \\
Q_{XT} &= W_b / (W_b - 1) \\
R_{XT} &= W_b / (W_b - 1)
\end{aligned}$$

being

$$\begin{aligned}
B_{E1} &= 1 \\
B_{E2} &= v_P / v_S \\
W_b &\text{ is a sensitivity factor} \\
N_I &= v_P \Delta t / \Delta x.
\end{aligned}$$

7. Higdon, Clayton and Engquist ABCs

In this case the coefficients $\{A_{pq}\}_{p,q=0,1,2}$ are expressed as:

$$\begin{aligned}
A_{00} &= 0 \\
A_{01} &= -(Q_{X2} + R_{X2}) \\
A_{02} &= -Q_{X2} R_{X2} \\
A_{10} &= -(Q_{T2} + R_{T2}) \\
A_{11} &= -(Q_{X2} R_{T2} + Q_{T2} R_{X2} + Q_{XT} + R_{XT2}) \\
A_{12} &= -(Q_{X2} R_{XT2} + R_{X2} Q_{XT}) \\
A_{20} &= -Q_{T2} R_{T2} \\
A_{21} &= -(Q_{T2} R_{XT2} + R_{T2} Q_{XT}) \\
A_{22} &= -Q_{XT} R_{XT2}
\end{aligned} \tag{9}$$

where:

$$\begin{aligned}
Q_{X2} &= (W_b(1 + N_I) - N_I) / ((1 + N_I) * (1 - W_b)) \\
R_{X2} &= (1 - \omega_{CFL}) / \omega_1 \\
Q_{T2} &= (W_b(1 + N_I) - 1) / ((1 + N_I) * (1 - W_b)) \\
R_{T2} &= -(1 - \omega_{CFL}) / \omega_1 = -R_{X2} \\
R_{XT2} &= -1
\end{aligned}$$

being

$$\begin{aligned}
\omega_{CFL} &= v_S \Delta t / \Delta x \text{ (i.e., the Courant–Friedrichs–Lewy ratio)} \\
\omega_1 &= 1 + \omega_{CFL}.
\end{aligned}$$

8. Liu and Archuleta ABCs

Liu and Archuleta (2000; personal communication) express the coefficients $\{A_{pq}\}_{p,q=0,1,2}$ as:

$$\begin{aligned}
A_{00} &= 0 \\
A_{01} &= H_{1X} \\
A_{02} &= 0 \\
A_{10} &= C_{1T} + H_{1T} \\
A_{11} &= C_{XT} + H_{XT} - H_{1X} C_{1T}
\end{aligned} \tag{10}$$

$$\begin{aligned}
A_{12} &= -H_{1X} C_{XT} \\
A_{20} &= -H_{1T} C_{1T} \\
A_{21} &= -H_{XT} C_{1T} - H_{1T} C_{XT} \\
A_{22} &= -H_{XT} C_{XT}
\end{aligned}$$

where:

$$\begin{aligned}
H_{1X} &= (\omega_{CFL} - W_b \omega_1) / (\omega_1 (1 - W_b)) \\
H_{1T} &= (1 - W_b \omega_1) / (\omega_1 (1 - W_b)) \\
H_{XT} &= W_b / (1 - W_b) \\
C_{1T} &= 1 - N_I \\
C_{XT} &= N_I
\end{aligned}$$

9. Peng and Toksöz ABCs

Peng and Toksöz (1994, 1995) introduced an Optimal ABC (also named OABC), which, as the authors showed, has less artificial reflections than Reynolds and Higdon ABCs (namely, reflection coefficients are about 10 to 30 dB less in magnitude). In this scheme we have a more complex expressions for coefficients $\{A_{pq}\}_{p,q=0,1,2}$:

$$\begin{aligned}
A_{00} &= 0 \\
A_{01} &= r_0(0,1) + R r_1(0,1) \\
A_{02} &= r_0(0,2) + R r_1(0,2) \\
A_{10} &= r_0(1,0) + R r_1(1,0) \\
A_{11} &= r_0(1,1) + R r_1(1,1) \\
A_{12} &= r_0(1,2) + R r_1(1,2) \\
A_{20} &= r_0(2,0) + R r_1(2,0) \\
A_{21} &= r_0(2,1) + R r_1(2,1) \\
A_{22} &= r_0(2,2) + R r_1(2,2)
\end{aligned} \tag{11}$$

where:

$$\begin{aligned}
t^+ &= \Delta \tilde{X} \cos(\theta^+), \text{ being } \theta^+ \text{ the incidence angle for which the } P \text{ wave to } P \text{ wave reflection coefficient} \\
&\text{ is zero (see equation (2) in Peng and Toksöz, 1995) and } \Delta \tilde{X} \text{ is the dimensionless} \\
&\text{ grid size (} \Delta \tilde{X} = (\omega/v_P) \Delta x \text{ and } \Delta \tilde{X} = (\omega/v_S) \Delta x \text{ for a maximum } P \text{ and } S \text{ wave} \\
&\text{ absorption, respectively; } \omega \text{ is an input-given angular frequency)} \\
t^- &= \Delta \tilde{X} \cos(\theta^-), \text{ being } \theta^- \text{ the incidence angle for which the } S \text{ wave to } S \text{ wave reflection coefficient} \\
&\text{ is zero (see equation (5) in Peng and Toksöz, 1995)} \\
R_z &= \cos(\Delta \tilde{t}), \text{ being } \Delta \tilde{t} \text{ the dimensionless time step (} \Delta \tilde{t} = \omega \Delta t \text{)} \\
I_z &= \sin(\Delta \tilde{t}) \\
R_x &= \cos(t^+ + t^-) \\
I_x &= \sin(t^+ + t^-) \\
R_y &= -(\cos(t^+) + \cos(t^-)) \\
I_y &= -(\sin(t^+) + \sin(t^-)) \\
\Delta &= 1 / \{ [R_y + I_y + 2R_z] * [(R_x R_z - I_x I_z) + (R_x I_z + R_z I_x) - R_z + I_z] + \\
&\quad [1 - R_x - I_x] * [2 + (R_y R_z - I_y I_z) + (R_y I_z + R_z I_y)] \}
\end{aligned}$$

$$\begin{aligned}
r_1(1,0) &= (1 - R_z) * [(R_x R_z - I I_z) + (R_x I_z + R_z I_x) - R_z + I_z] * \Delta \\
r_1(0,2) &= (1 - R_z) (1.0 - R_x - I_x) * \Delta \\
r_1(0,1) &= -0.5 - r_1(1,0) \\
r_1(1,1) &= 1 - 2r_1(0,2) \\
r_1(0,0) &= 0 \\
r_1(2,2) &= 0 \\
r_1(1,2) &= r_1(1,0) \\
r_1(2,0) &= r_1(0,2) \\
r_1(2,1) &= r_1(0,1) \\
r_0(0,2) &= - \{ [R_z + I_z - (R_x R_z + I I_z) + (R_x I_z - R_z I_x)] * [R_y + I_y + 2R_z] + \\
&\quad [1 + R_z + (R_y R_z + I I_z) - (R_y I_z - R_z I_y)] * [1 - R_x - I_x] \} * \Delta \\
r_0(1,0) &= \{ [1 + R_z + (R_y R_z + I I_z) - (R_y I_z - R_z I_y)] * [(R_x R_z - I I_z) + (R_x I_z + R_z I_x) - R_z + I_z] + \\
&\quad [R_z + I_z - (R_x R_z + I I_z) + (R_x I_z - R_z I_x)] * [2 + (R_y R_z - I I_z) + (R_y I_z + R_z I_y)] \} * \Delta \\
r_0(0,1) &= 0.5 - r_0(1,0) \\
r_0(1,1) &= 1 - 2r_0(0,2) \\
r_0(2,2) &= -1 \\
r_0(1,2) &= r_0(1,0) \\
r_0(2,0) &= r_0(0,2) \\
r_0(2,1) &= r_0(0,1) \\
R &= - \sum_{n=0}^2 \sum_{m=0}^2 r_0(n,m) r_1(n,m) / \sum_{n=0}^2 \sum_{m=0}^2 r_1(n,m) r_1(n,m)
\end{aligned}$$

10. Summary

In the modeling of the phenomena occurring during a seismic rupture there is the need to properly resolve the spatial and temporal scales of the process. This in turn requires the use of efficient, massively parallel and stable numerical algorithms to ensure an accurate solution at high frequencies. The computational resources nowadays available can result still insufficient for some specific applications, since the primary interest of the modeler is to avoid spurious reflections generated at the boundary of the computational domain, which is, by construction, bounded.

An efficient way to avoid such numerical artifacts is to preserve the original size of the model, without arbitrarily enlarge it, and to implement Absorbing Boundary Conditions (ABCs). When a propagating wave reaches (or approaches to) an absorbing boundary, then it is “absorbed” from it, in that the reflections from the boundary are suppressed (or significantly attenuated).

In this work we have presented a large number of ABCs that can be used in the numerical modeling of wave propagation, excited by a seismic rupture developing on a fault surface. The different conditions described in sections 3 to 9 can be easily incorporated into a FORTRAN code, by exploiting the compact notation presented in section 2.3 (equations (3) and (4)).

Another type of ABC which has not been mentioned above is represented by the Perfectly Matched Layers (PMLs). The PML concept was introduced by J.-P. Berenger for use with Maxwell’s equations, in a seminal paper (Berenger, 1994) and it has been subsequently extended to the field of elasticity (see Festa and Nielsen, 2003 and references therein). In principle, PMLs can provide orders-of-magnitude lower reflections than other ABCs conditions, do not loose efficiency at shallow angles and are notoriously effective even with surface waves. PMLs technically consist in an absorbing region rather than a boundary condition *per se*; therefore they are more complex to be implemented, since they require a finite number of nodes (usually 5 to 10). PMLs have been applied in Finite Difference, staggered grid codes and that are presently under evaluation to be implemented in a conventional grid scheme, such as that we are presently using (see section 1).

As every ABC, the conditions presented in this work — and the PMLs ABCs as well — are not *totally* absorbing, in that a small fraction of the reflected waves is still maintained and can potentially pollute the solutions of a numerical experiment.

The quantitative evaluation of the effectiveness, in some typical case studies, of all the ABCs presented above is certainly beyond the scope of the present study and it will be the subject of a paper in preparation. Here we have simply presented a large number of ABCs and we have explicitly indicated how they can be incorporated into a FORTRAN code. Since there is no best ABC which would be universally (i.e., in all wavefield configurations) both sufficiently stable and accurate, the modeler is highly recommended to be able to use several different formulations in its numerical simulations and finally to evaluate, depending on the specific problem, what is the optimal ABC.

Acknowledgements

Martin Galis is kindly acknowledged for fruitful, early discussions about Absorbing Boundary Conditions. I'm grateful to Angelo De Santis for a detailed review and for stimulating comments.

References

- Berenger, J (1994). A perfectly matched layer for the absorption of electromagnetic waves. *Journal of Computational Physics*, 114, 185–200, doi: 10.1006/jcph.1994.1159
- Bizzarri, A. (2009). Can flash heating of asperity contacts prevent melting?. *Geophys. Res. Lett.*, 36, L11304, doi: 10.1029/2009GL037335
- Bizzarri, A., Cocco, M. (2005). 3D dynamic simulations of spontaneous rupture propagation governed by different constitutive laws with rake rotation allowed. *Ann. Geophysics*, 48, No. 2, 279–299
- Bizzarri, A., Dunham, E. M., Spudich P. (2009). Coherence of Mach fronts during heterogeneous supershear earthquake rupture propagation: simulations and comparison with observations. *J. Geophys. Res.*, under review
- Bizzarri, A., Spudich, P. (2008). Effects of supershear rupture speed on the high-frequency content of *S* waves investigated using spontaneous dynamic rupture models and isochrone theory. *J. Geophys. Res.*, 113, B05304, doi:10.1029/2007JB005146
- Clayton, R., Engquist, B. (1977). Absorbing boundary conditions for acoustic anelastic wave equations. *Bull. Seism. Soc. Am.*, 67, 1529–1540
- Emerman, S. H., Stephen, R. A. (1983). Comment on “Absorbing boundary conditions for acoustic and elastic wave equations” by R. Clayton and B. Engquist. *Bull. Seism. Soc. Am.*, 73, 661–665
- Festa G., Nielsen, S. (2003). PML Absorbing Boundaries. *Bull. Seism. Soc. Am.*, 93, No. 2, 891–903
- Higdon, R. L. (1991). Absorbing boundary conditions for elastic waves. *Geophysics*, 56, 231–241
- Peng, C., Toksöz, M. N. (1994). An optimal absorbing boundary condition for finite difference modelling of acoustic and elastic wave propagation. *J. Acoust. Soc. Am.*, 95, 733–745
- Peng, C., Toksöz, M. N. (1995). An optimal absorbing boundary condition for elastic wave modelling. *Geophysics*, 60, 296–301
- Reynolds, A. C. (1978). Boundary conditions for the numerical solution of wave propagation problems. *Geophysics*, 43, 1099–1110.

Coordinamento editoriale e impaginazione

Centro Editoriale Nazionale | INGV

Progetto grafico e redazionale

Laboratorio Grafica e Immagini | INGV Roma

© 2009 INGV Istituto Nazionale di Geofisica e Vulcanologia

Via di Vigna Murata, 605

00143 Roma

Tel. +39 06518601 Fax +39 065041181

<http://www.ingv.it>



Istituto Nazionale di Geofisica e Vulcanologia